Rev.Adv.Mater.Sci. 18(2008) 159-163

ATOMIC PACKING EFFICIENCY OF THE COMPETING CRYSTAL PHASES AND GLASS FORMING ABILITY FOR THE Cu AND Ti BASED ALLOYS

G. J. Hao, Y. Zhang, J.P. Lin and G. L. Chen

State Key Laboratory for Advanced Metals and Materials, University of Science and Technology Beijing, Beijing 100083, China

Received: March 29, 2008

Abstract. The effects of yttrium addition on the glass forming ability (GFA) of the Cu- and Ti-based alloys have been investigated. It is found that yttrium addition can dramatically enhance GFA in Cu-based alloy and a Ti-base alloys, and minor addition of yttrium, can destabilize the $Cu_{10}Zr_7$, CuZr, and Laves phase in Cu- and Ti-based alloys, respectively. The atomic level strain energy is closely related to the atomic packing efficiency of the precipitated crystals. The prediction correlates well with the experimental results that less yttrium addition is needed to suppress the precipitation of crystal phase with the higher atomic packing efficiency.

1. INTRODUCTION

Due to the considerable scientific and technological importance of bulk metallic glasses (BMGs), a large number of efforts have been devoted to investigate the glass-forming ability (GFA) of metallic alloys [1-3]. As a result, hundreds of bulk glass-forming alloys with diameters up to several centimeters have been prepared. However, the engineering commercialization of these BMGs as structural materials is hindered by their limited GFA, low thermal stability and unsatisfactory manufacturability. Recently, it was reported that microalloying or minor alloying additions were very effective in increasing GFA, enhancing thermal stability and improving magnetic and mechanical properties for some BMGs [4].

Yttrium has been widely used in bulk metallic alloys as a minor addition element, e.g. Fe-based [5], Zr-based [6], and Cu-based [7] BMGs, the addition of a small amount of yttrium was found to be an effective method to improve the GFA. The effect of Y on glass formation was attributed to the following: 1) Y scavenged the oxygen impurity from alloy, via the formation of innocuous yttrium oxides; 2) Y adjusted the compositions closer to the eutectic and thus lowered their liquidus temperature; 3) there were appropriate atomic-size mismatch and large negative heat of mixing between Y and existing constitutive elements; and 4) Y destabilizes the crystalline phase [8] or acts as a principal element [9].

On the other hand, to make bulk glasses, one must frustrate the process of crystallization. Glass formation is always a competing process between amorphous and crystalline phases. Thus, studying the competing crystalline phases is necessary to understand the effect of Y on the GFA.

2. EXPERIMENTS

The master alloys were prepared by arc melting the constituent elements-Cu, Ti, Zr, Al, Ni, Be, and Y with commercial grade purities of 99.9%, 99.3%, 99.4, 99.7%, 99.9%, 99.8%, and 99.5%, respectively in a Ti gettered high-purity argon atmosphere.

Corresponding author: Yong Zhang, e-mail: drzhangy@skl.ustb.edu.cn

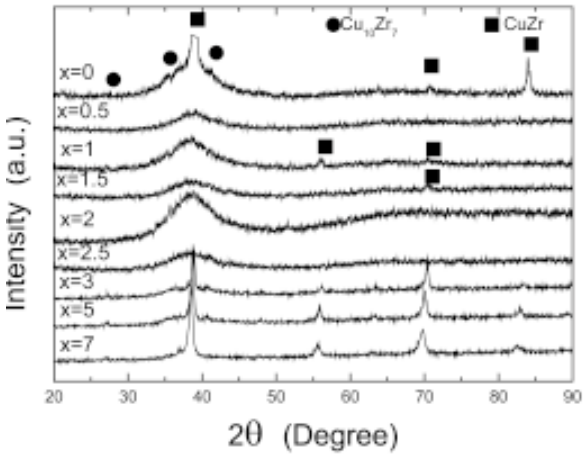

Fig. 1. X-ray diffractograms of as-cast rods of $(Cu_{0.48}Zr_{0.48}Al_{0.04})_{100-x}Y_x$ (at.%) illustrating the yttrium effect on glass formation, the crystal phases are mainly CuZr and $Cu_{10}Zr_7$ phases.

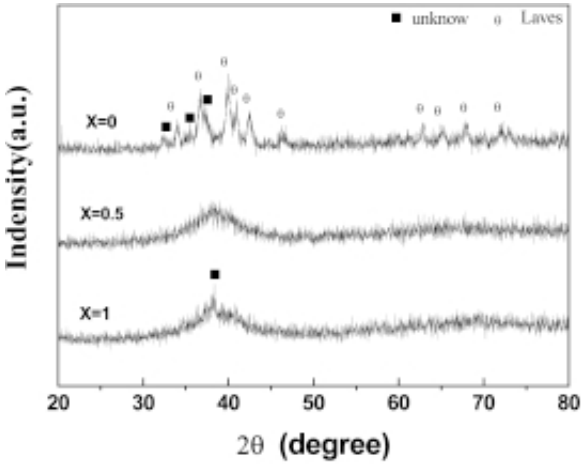

Fig. 2. XRD patterns of the central part of as-cast 5-mm ingots for a model alloy system $(Ti_{40}Zr_{25}Be_{20}Cu_{12}Ni_3)_{100-X}Y_X$ (x = 0, 0.5, 1) illustrating the yttrium effect on glass formation. The mainly competing phase was identified as a hexagonal Laves phase with lattice constants of a = 0.52 nm and c = 0.86 nm.

Their nominal compositions are $(Cu_{0.48}Zr_{0.48}Al_{0.04})_{100-x}Y_x$ (x = 0~7, atomic percent), $(Ti_{0.4}Zr_{0.25}Be_{0.2}Cu_{0.12}Ni_{0.3})_{100-X}Y_X$ (x=0~5, atomic percent), and each ingot was melted at least three times in order to obtain chemical homogeneity. The ingots were then remelted under high vacuum (10^{-4} Pa) and cast by suction of the melt into a copper mold to obtain 70 mm-long cylindrical rods of 3 mm and 5 mm in diameter. The structure of the cylindrical alloys (cross-sectional surface) was characterized by X-ray diffraction (XRD) using CuK_α radiation, and the thermal properties associated with glass transition and crystallization of the amorphous phase were measured using differential scanning calorimetry (DSC; Perkin Elmer DSC7). DSC traces were monitored during continuous heating from 373 to 1073K using a low constant heating rate of 10 K/min.

3. RESULTS

3.1 Effect of yttrium on microstructures

Rods of $(Cu_{0.48}Zr_{0.48}Al_{0.04})_{100-x}Y_x$ alloys were cast with 3mm diameter. As shown by XRD of rod cross-sections (Fig. 1), sample with 2% yttrium addition is amorphous, while those with x<2% and x>2% are partially crystalline. The amorphicity samples were further checked by transmission electron microscopy (TEM), apart from isolated 1-2 nm particles (small nanocrystalls do not appear on XRD and SEM), there was no evidence of crystalline phases. As shown in Fig. 1, in the alloys with no yttrium addition the key phases were identified as $Cu_{10}Zr_7$ and CuZr. With 1% yttrium addition, only two strong crystal peaks are observed. The two strong peaks agree well with CuZr phase. Similarly, with the further increase of yttrium addition (X>2), some sharp crystalline peaks superimposed on the main halo are observed, and the crystalline phases were identified as $Cu_{10}Zr_7$ and CuZr.

The high cooling rate of copper mold casting may lead to the eutectic coupled zone being skewed towards the primary phase with higher slope of liquidus line, and also the optimum glass formation being shifted to the off-eutectic [10]. Our previous work has well illustrated this point [11] and the XRD data is consistent with the microstructure examined by SEM. The microstructure of $(Cu_{0.48}Zr_{0.48}Al_{0.04})_{(100-x)}Y_x$ alloy without yttrium addition is a mixture of Primary (CuZr) + eutectic (CuZr+$Cu_{10}Zr_7$). The eutectic of CuZr and $Cu_{10}Zr_7$ laminar structure presents circle like morphology, and the cross like phase in the center of the circle is the primary phase of CuZr [11]. Thus, we can conclude that with 1 at.% yttrium addition suppress eutectic clusters via Y destabilize $Cu_{10}Zr_7$ phase.

Then, 2 at.% Y suppress both $Cu_{10}Zr_7$ and CuZr precipitates as shown in Fig. 1.

Fig. 2 shows the XRD patterns of the sectional part of 5-mm suction-cast rod samples for the alloy $(Ti_{0.4}Zr_{0.25}Be_{0.2}Cu_{0.12}Ni_{0.3})_{100-X}Y_X$ (x= 0, 0.5, 1). It clearly illustrates the yttrium effect on glass formation. Without the addition of yttrium the specimen shows some sharp crystalline peaks, no broad scattering peak, suggesting that this sample is fully crystalline, the mainly crystalline phase was identified as a hexagonal Laves phase with lattice constants of a = 0.523 nm and c = 0.859 nm, which contains Ti, Zr, and Cu elements. For the alloy with 0.5 at.% Y, only a broad scattering peak without any evidence of crystalline phase was observed, indicating that this 5-mm as-cast ingot consists of mostly amorphous structure, as shown in Fig. 2 (x=0.5). Thus, only 0.5 at.% of yttrium addition can suppress the precipitation of Laves phase and enhance GFA of this amorphous alloy. However with the further increase of the amount of yttrium, some sharp crystalline peaks superimposed to the main halo are observed, implying that these samples have partially amorphous structure, as shown in Fig. 2 (x=1).

3. 2 Effect of yttrium on the thermal behavior

Fig. 3a shows the dependence of liquidus temperature T_l and melting temperature T_m on Y content. It was found a small change of liquidus temperature and melting temperature (solidus temperature) with yttrium content, and the lowest liquidus temperature is not consistent with the best GFA composition (x=2). The reduced glass transition temperature T_{rg}(=T_g/T_l), GFA parameter γ (=$T_x/(T_g+T_l)$, here T_x is onset crystallization temperature) and supercooled liquid region ΔT_x(=T_x-T_g) as a function of Y content are shown in Figs. 3b and 3c). T_{rg}, γ, and ΔT_x decrease slightly with increasing Y content, which indicates that the effect of minor Y addition on these thermal parameters of the Cu-based alloy is small. Table 1 summarizes the T_g, T_m, T_l, T_{rg}, ΔT_x, g and T_x values for the Cu-based alloys. According to Table 1, T_{rg} and γ of the best GFA alloy with 2 at.% Y addition exhibits the highest value in all of alloys. However, it should be noted that the alloy exhibiting the lowest GFA (with no Y addition) indicates the second highest T_{rg} and γ.

The effect of Y on the GFA of Ti-based metallic alloys with the composition $(Ti_{0.4}Zr_{0.25}Be_{0.2}Cu_{0.12}Ni_{0.3})_{100-X}Y_X$ was investigated in our previous study [12]. The investigation indicated

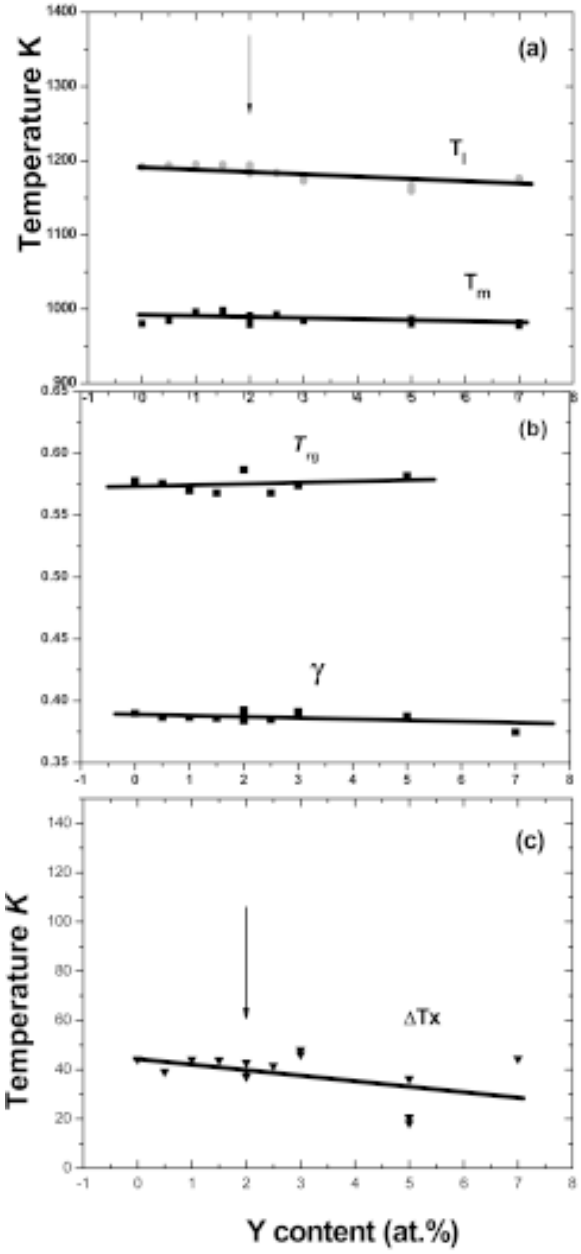

Fig. 3. The thermal parameters as a function of Y content along $(Cu_{0.48}Zr_{0.48}Al_{0.04})_{100-x}Y_x$ (at.%), and the best GFA of alloy be marked by arrow.

0.5 at.% Y addition can suppress Laves phase precipitation and improve the GFA of alloy. The alloy with 0.5 at.% Y addition exhibits the second highest value of T_{rg}=0.65, but has the highest GFA, and the highest T_{rg} value obtained for the 2 at.% Y addition alloy does not form a fully amorphous phase. Thus, T_{rg} is not the key parameter in this amorphous alloy. A large ΔT_x value may indicate that the supercooled liquid can exist in a wide temperature range without crystallization and has a high

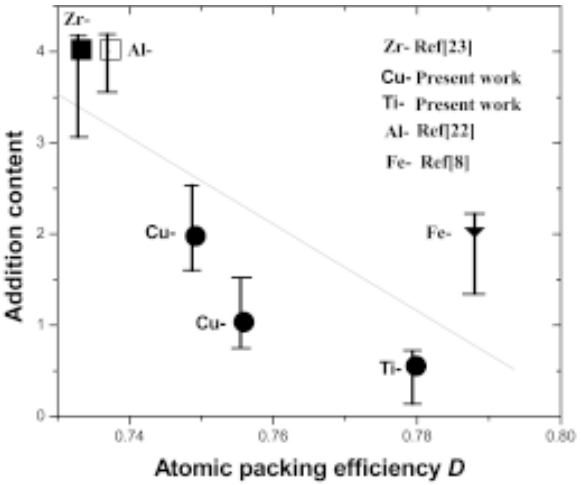

Fig. 4. Dependence of effective addition content on crystal atomic packing efficiency *D* observed in some bulk metallic glasses.

resistance to the nucleation and growth of crystalline phases. However, for the alloy with 0.5 at.% Y, the supercooled liquid range ΔT_x is smaller than that of the alloy $Ti_{45}Zr_{25}Be_{20}Cu_{12}N_{i3}$ reported [13], and no relationship with GFA in the least.

4. DISCUSSIONS

Computer simulation [13], topological studies [14,15], and empirical rules [2] drawn from experimental results have all shown that certain atomic-size mismatch and atomic packing efficiency may enhance GFA of a system. D.B. Miracle [15] calculated a set of preferred values R^* for the ratio of the solute atom radius to the solvent atom radius in the Table 1, and at which the local packing efficiency (defined in terms of a coordination number) assumes its maximum. In the present system, the atomic radii of the component atoms are Y, 1.74 Å; Zr, 1.58 Å; Al, 1.43 Å, and Cu, 1.27 Å, respectively. Therefore, $R_{Zr/Cu}$=1.244, $R_{Al/Cu}$=1.126, and $R_{Y/Cu}$=1.37. Comparing these values with the critical values listed in Ref [15], good agreement can be found that R^*_{17}(1.248), R^*_{15}(1.116), and R^*_{19}(1.373). Therefore, the present combination of atomic sizes can produce an efficiently packed local structure, which is often associated with low energy and high viscosity of liquids.

D.B. Miracle [16] proposed a topological model for metallic glass formation through destabilization of the host crystalline lattice by substitutional and/or interstitial solute elements, and suggested that the crystalline lattice is destabilized leading to amorphization when solute elements produce a critical internal strain required to change local coordination numbers. When a large Y atom substitutes a relatively small Zr or Cu atom, internal strain will be induced. In the present work, we introduced crystal distortion energy, ΔE to explain the effect of Y on glass-forming ability. According to Fig. 1, the crystallization peaks alterative to left with increasing yttrium addition, indicating an increasing of the interplana spacing. The above analysis indicates that the size of CuZr crystal cell increases with yttrium addition. Studying the negative heat of mixing (HM) among the constituent elements, the HM values [17] of Y-Cu and Zr-Cu are -22 and -23 kj/mol, respectively, which indicates that H_{mix} of Y-Cu and ΔH_{mix} of Zr-Cu is very similar. Therefore, given the values of the two parameters ΔH_{mix} and atomic size, Y may substitute the larger atoms of Zr in CuZr and $Cu_{10}Zr_7$, and thus increase the crystal cell size and induce the crystal distortion energy. By taking the crystal distortion energy into account [18,19], the crystal stability would decrease, and then the free energy of the competing crystal phase would increase. From Fig. 3 and Table 1, T_l , T_m, and T_g are less dependent on the minor yttrium addition when Y content less than 2%. These indicate that the chemical effect between the solvent and added Y is small and these thermodynamic parameters fail to explain the order of magnitude difference in critical cooling rates of these Cu-based bulk amorphous alloys. Therefore, we assume that the crystal distortion energy (strain energy) is the main parameter to determine the crystal stability in present system, and the chemical effect between the solvent and solute (addition) atoms do not influence the location of the solute atom and, therefore, the Gibbs free energy change will be equal to the difference of crystal distortion energy induced by Y substitution of Zr. The strain energy is closely related to the crystal structure, especially the atomic packing efficiency [12,20]. The CuZr phase has a B2 structure, and $Cu_{10}Zr_7$ phase belongs to Aba2 space group, and has Pearson's symbol oC68, with $Ni_{10}Zr_7$ type [21]. It is obvious that the atomic packing efficiency of $Cu_{10}Zr_7$ phase is higher than that of the CuZr phase. Thus, for destabilizing the crystal phases, the needed yttrium content *x* will be higher for CuZr phase than that for $Cu_{10}Zr_7$ phase. This agrees well with the XRD results. With 1 at.% Y addition, $Cu_{10}Zr_7$ phase was suppressed in the alloy, while when Y content increases to 2 at.%, both $Cu_{10}Zr_7$ and CuZr phases were suppressed.

The atomic packing efficiency of Laves phase ($MgZn_2$ type) is also calculated. It is found that the Laves phase presents highest atomic packing density 0.78 in these crystal structures. Therefore, it indicate that the yttrium content is closely related to the efficiency of space filling of competing phases. While the series of atomic packing density are: D(Laves) >D($Cu_{10}Zr_7$) > D(CuZr), thus the effective yttrium addition is x(0.5 at.%) < x(1 at.%) < x(2 at.%). Fig. 4 shows the effective addition content as a function of competing crystal atomic packing efficiency, showing a rough correlation between the yttrium content between atomic packing efficiency. It should be noted that the chemical effects are not considered in this discussion. Thus, the observed rough correlation reveals that competing crystal structure is closely related to the value of addition content which destabilize crystalline phases.

5. CONCLUSIONS

For $(Cu_{0.48}Zr_{0.48}Al_{0.04})_{100-x}Y_x$ and $(Ti_{0.4}Zr_{0.25}Be_{0.2}Cu_{0.12}Ni_{0.03})_{100-x}Y_x$ alloys, the liquidus temperature changes slightly with yttrium addition and the GFA does not correlate well with the ΔTx, T_{rg}, and γ parameters. Y addition will induce crystal distortion energy when it substitutes the Zr due to its larger atomic size, the nucleation energy barriers of CuZr, $Cu_{10}Zr_7$ and Laves phase will increase, and then improve the GFA. As distortion energy is proportional to the yttrium content and the atomic packing density, the amount of effective yttrium addition needed to supress nucleation of crystalline phase will decrease with increasing of the crystal atomic packing efficiency.

ACKNOWLEDGEMENTS

The authors would like to acknowledge financial support by the National Natural Science Foundation of China NNSFC (No.50571018), and from the Program for New Century Excellent Talents in Universities (NCET) of China.

REFERENCES

[1] A.L. Greer // *Science* **267** (1995)1947.
[2] A. Inoue // *Acta Mater* **48** (2000) 279.
[3] W. H. Wang, C. Dong and C. H. Shek // *Mater. Sci. Eng R* **44** (2004) 45.
[4] Z. P. Lu and C. T. Liu // *J Mater. Sci.* **39** (2004) 3965.
[5] Z. P. Lu, C. T. Liu and W. D. Porter // *Appl. Phys. Lett.* **83** (2003) 2581.
[6] Y. Zhang, M.F. Pan, D. Q. Zhao, R. J. Wang and W. H. Wang // *Mater. Trans., JIM* **41** (2000)1410.
[7] D. H. Xu, G. Duan and W. L. Johnson // *Phys. Rev. Lett.* **92** (2004) 245504.
[8] V. Ponnambalam, S.J. Poon and G. J. Shiflet // *J Mater Res* **19** (2004) 1320.
[9] J.Zhang, H. Tan, Y. P. Feng and Y. Li // *Scripta Mater* **53** (2005)183.
[10] Y. Zhang, W. Xu, H. Tan and Y. Li // *Acta Mater* **53** (2005) 2607.
[11] J. Chen, Y. Zhang and G. L. Chen // *Scripta Mater* **54** (2006)1351.
[12] G. J. Hao, Y. Zhang, J. P. Lin, Y.L. Wang, Z. Lin and G. L. Chen // *Mater. Lett.* **60** (2006) 1256.
[13] H. J. Lee, T. Cagin, W. L. Johnson and W. A. Goddard // *J. Chem. Phys.* **119** (2003) 9858.
[14] T. Egami and Y. Waseda // *J. Non-Cryst. Solids* **64** (1984)113.
[15] D. B. Miracle, W. S. Sanders and O. N. Senkov // *Philos. Mag.* **83** (2003) 2409.
[16] D. B. Miracle and O. N. Senkov // *Mater. Sci. Eng. A* **347** (2003) 50.
[17] F. R. de Boer // *Amsterdam: North- Holland.* **351** (1989) 375.
[18] K. Lu and Y. Li // *Phys Rev Lett* **80** (1998) 4474.
[19] V.M. Fokin, E.D. Zanotto, J. W. P. Schmelzer and O. V. Potapov // *J. Non-Crys. Sol.* **351** (2005)1491.
[20] G.L Allen, W.W. Gile and W.A. Jesser // *Acta Metall.* **28** (1980)1695.
[21] Y. Zhang, J. Chen, G. L. Chen and X. J. Liu // *Appl. Phys. Lett.* **89** (2006) 131904.
[22] A. Revesz, L. K. Varga, P. M. Nagy, J. Lendvai and I. Bakonyi // *Mater. Sci and Eng A* **351** (2003) 160.
[23] W. H. Wang, Z. Bian, Ping Wen, Yong Zhang, M. X. Pan and D. Q. Zhao // *Intermetallics* **10** (2002) 1249.